Proper Positioning of the Nicotinamide Ring Is Crucial for the *Ascaris suum* Malic Enzyme Reaction†

Deniz F. Aktas and Paul F. Cook*

Department of Chemistry and Biochemistry, University of Oklahoma, 620 Parrington Oval, Norman, Oklahoma 73019

Received November 13, 2007; Revised Manuscript Received December 20, 2007

ABSTRACT: The mitochondrial NAD−malic enzyme catalyzes the oxidative decarboxylation of malate to pyruvate and CO_2. The role of the dinucleotide substrate in oxidative decarboxylation is probed in this study using site-directed mutagenesis to change key residues that line the dinucleotide binding site. Mutant enzymes were characterized using initial rate kinetics, and isotope effects were used to obtain information on the contribution of these residues to binding energy and catalysis. Results obtained for the N479 mutant enzymes indicate that the hydrogen bond donated by N479 to the carboxamide side chain of the nicotinamide ring is important for proper orientation in the hydride transfer step. The stepwise oxidative decarboxylation mechanism observed for the wt enzyme changed to a concerted one, which is totally rate limiting, for the N479Q mutant enzyme. In this case, it is likely that the longer glutamine side chain causes reorientation of malate such that it binds in a conformation that is optimal for concerted oxidative decarboxylation. Converting N479 to the shorter serine side chain gives very similar values of K_{NAD}, K_{malate}, and isotope effects relative to wt, but V/E_t is decreased 2 000-fold. Data suggest an increased freedom of rotation, resulting in nonproductively bound cofactor. Changes were also made to two residues, S433 and N434, which interact with the nicotinamide ribose of NAD. In addition, N434 donates a hydrogen bond to the β-carboxylate of malate. The K_{NAD} for the S433A mutant enzyme increased by 80-fold, indicating that this residue provides significant binding affinity for the dinucleotide. With N434A, the interaction of the residue with malate is lost, causing the malate to reorient itself, leading to a slower decarboxylation step. The longer glutamine and methionine side chains stick into the active site and cause a change in the position of malate and/or NAD resulting in more than a 10^4-fold decrease in V/E_t for these mutant enzymes. Overall, data indicate that subtle changes in the orientation of the cofactor and substrate dramatically influence the reaction rate.

Malic enzyme is a pyridine nucleotide-linked β-hydroxy-acid oxidative decarboxylase, which catalyzes the divalent metal ion (Mg^{2+} or Mn^{2+}) dependent conversion of L-malate to pyruvate and CO_2, with concomitant reduction of NAD(P) to NAD(P)H (*1*−*3*).[1]

The malic enzyme was first found in pigeon liver and was a cytosolic enzyme that required NADP as an oxidant (*1*). The *Ascaris suum* mitochondrial NAD-malic enzyme (E.C. 1.1.1.39) was isolated from the anaerobic parasitic nematode in 1956 (*4*). Malic enzyme plays an important role in the energy metabolism of the nematode. L-Malate is the product of anaerobic glycolysis and malic enzyme in the mitochondrion is responsible for producing NADH, which is the main source of ATP synthesis via site I oxidative phosphorylation (*5*−*7*).

On the basis of initial velocity, product inhibition, isotope partitioning, and deuterium isotope effect studies (*8*−*10*), a steady-state random kinetic mechanism was proposed for the *A. suum* malic enzyme, with the requirement that Mg^{+2} adds prior to malate. A general acid−base mechanism was proposed on the basis of the pH dependence of kinetic parameters and isotope effects (*10*, *11*). Recently, according to Karsten et al. (*12*), a catalytic triad, involving residues K199, Y126, and D294, was shown to be responsible for the acid−base chemistry in the *Ascaris* enzyme (Figure 1). The catalytic pathway, comprising a conformational change, followed by hyride transfer and decarboxylation, contributes to rate limitation of the overall reaction. In addition, malate is sticky and has an off-rate constant from the central E−NAD−Mg−malate complex equal to the net rate constant for catalysis (*9*, *10*), while at saturating concentrations of reactants an isomerization of E−NAD also contributes to rate limitation (*13*).

The aim of this study was to determine the possible functional roles of several residues in the dinucleotide binding site. Site-directed mutagenesis has been used as a probe of the NAD and NADH binding sites. Residues N479, S433, and N434 were mutated to a number of different amino acids to alter the side chain functionality. The mutant

† This work was supported by a grant to P.F.C. from NSF (MCB 0091207) and the Grayce B. Kerr endowment to the University of Oklahoma to support the research of P.F.C..

* Corresponding author. Phone: 405-325-4581. Fax: 405-325-7182. E-mail: pcook@ou.edu.

[1] Abbreviations: Ches, 2-(*N*-cyclohexlamino)ethanesulfonic acid; Hepes, *N*-(2-hydroxyethyl)piperazine-*N*′-2-ethanesulfonic acid; IPTG, isopropyl β-D-1-thiogalactopyranoside; LDH, lactate dehydrogenase; NAD(P), nicotinamide adenine dinucleotide (2′-phosphate), the plus sign was omitted for convenience; TDH, tartrate dehydrogenase; wt, wild type.

10.1021/bi702261m CCC: $40.75
Published on Web 01/24/2008

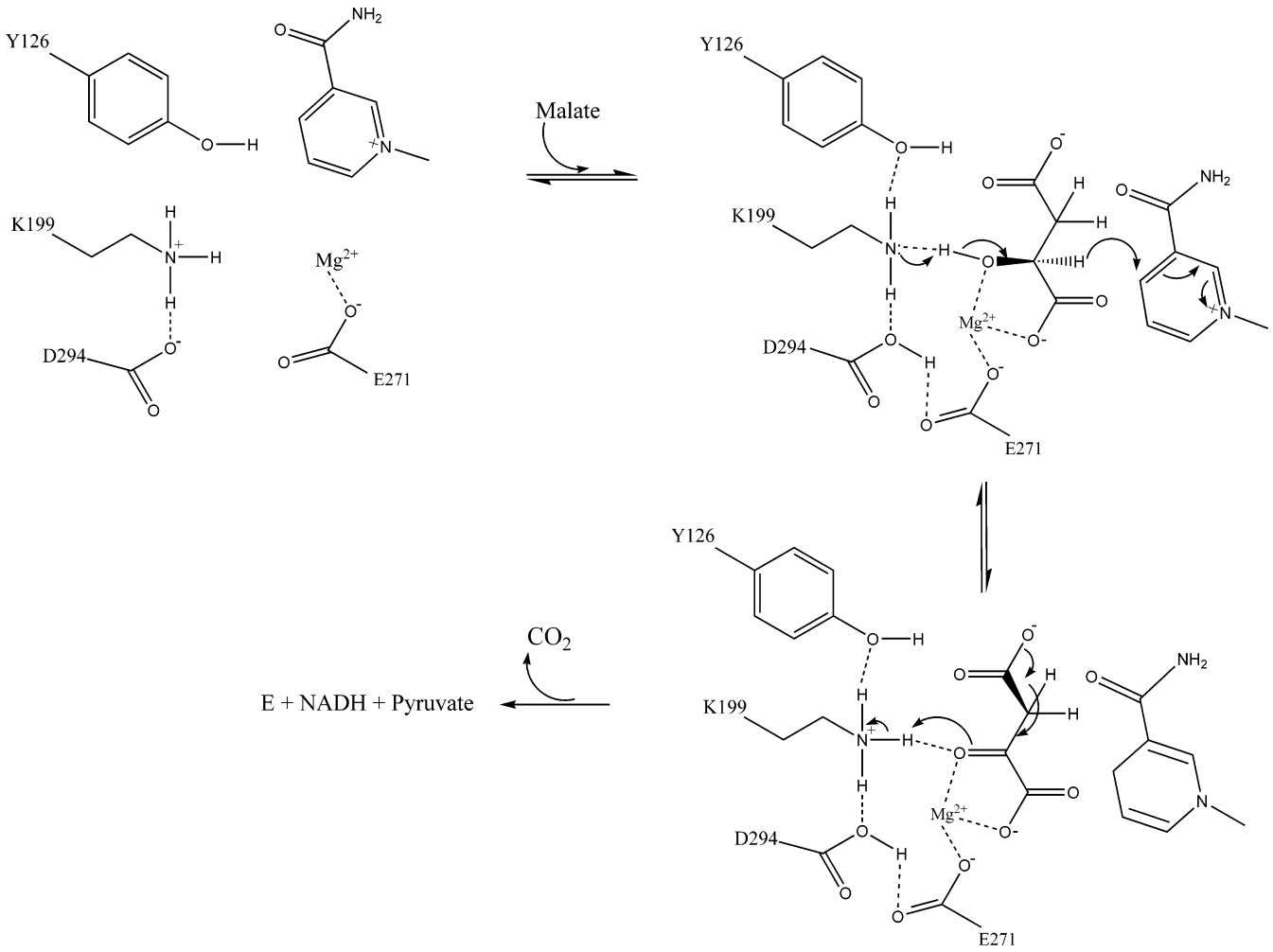

FIGURE 1: Proposed general acid−base chemical mechanism for *Ascaris suum* malic enzyme.

enzymes were characterized by initial rate, inhibition, and isotope effect studies. The contribution to binding energy and catalysis of the groups that interact with NAD and NADH have been investigated and the implications to the catalytic mechanism are discussed.

MATERIALS AND METHODS

Chemicals and Enzymes. Malate, NAD, and NADH were obtained from USB. Hepes and Ches buffers were from Research Organics, while Pipes buffer and fumarate were purchased from Sigma. Magnesium sulfate and manganese sulfate were obtained from Fisher Scientific. Sodium borodeuteride (98 atom %) was from Aldrich and IPTG was from GoldBio Tech. The QuikChange site-directed mutagenesis kit was from Stratagene. The recombinant *A. suum* malic enzyme used in these studies has a 6-histidine N-terminal tag, and both the wild type and mutant enzymes were prepared and purified as described previously (*14*). Protein concentrations were obtained using the method of Bradford (*15*). All other chemicals and reagents used were obtained commercially and were of the highest purity available.

Malate-2-d. Malate-2-*d* was synthesized by the reduction of oxaloacetate with sodium borodeuteride (*16*). A solution of 40 mM oxaloacetate was prepared, and its pH was adjusted to pH 7 with KOH. Sodium borodeuteride was added to a final concentration of 40 mM to this solution and allowed to incubate at room temperature for 1 h, and the pH was then adjusted to 5 with acetic acid. Pipes buffer and NAD were added to final concentrations of 25 mM and 0.2 mM, respectively, and the pH was adjusted to 7 with KOH. KCl (30 mM), $MnSO_4$ (1 mM), TDH (170 units), and LDH (50 units) were added, and the solution was allowed to incubate at room temperature for 48 h to remove D-malate-2-*d*. The amount of the remaining D-malate-2-*d* in the solution was determined by end-point assay using tartrate dehydrogenase. The end-point assay contained 100 mM Ches, pH 8.5, 1 mM $MnSO_4$, 1 mM NAD, 30 mM KCl, ~1 unit TDH, and 5 μL of the synthesis solution. More than 95% of the D-malate-2-*d* was removed. The pH of the resulting solution was adjusted to 5 with perchloric acid, and activated charcoal was added to remove the dinucleotides. After filtration and concentration via rotary evaporation, L-malate-2-*d* was purified by Dowex AG-1-X8 column chromatography. The L-malate-2-*d* concentration was determined by end-point assay containing 1.5 units of wild type *A. suum* malic enzyme, 100 mM Ches, pH 8.5, 1 mM $MnSO_4$, 1 mM NAD, 2 mM fumarate, and ~0.1 mM L-malate-2-*d*.

Enzyme Assays. Enzyme assays were carried out at 25 °C in 1 cm cuvettes using a Beckman DU640 UV−visible spectrophotometer. In the direction of oxidative decarboxylation of malate, malic enzyme activity was measured at varying concentrations of L-malate, divalent metal ion, and

NAD as indicated in the text. The nonvaried substrate was maintained at a concentration at least 10 times its K_m value, and reaction mixtures were maintained at pH 7 with 100 mM Hepes buffer. The reaction was followed at 340 nm to monitor the production of NADH (ϵ_{340}, 6220 M^{-1} cm^{-1}). Malic enzyme uses the uncomplexed form of the divalent metal ion and substrates, and corrections for chelate complexes were made using the following dissociation constants: Mg−malate, 25.1 mM; Mn−malate 5.4 mM; Mg−NAD 19.6 mM; Mn−NAD and Mn−NADH 12.6 mM (*8*). All substrate concentrations reported in the text refer to the uncomplexed concentrations of substrates and divalent metal ion.

The primary kinetic deuterium isotope effects were determined by direct comparison of initial velocities using 100 mM Hepes, pH 7, saturating concentrations of NAD and metal ion, and varied concentrations of L-malate-2-*h*(*d*). The inhibition constant for NADH was obtained by measuring the initial rate as a function of NAD with metal ion and malate fixed at their respective K_m values and at different concentrations of NADH, including zero.

^{13}C Kinetic Isotope Effects. The ^{13}C isotope effects on the malic enzyme reaction were determined using the natural abundance of ^{13}C in the substrate as the label (*17*). Both high-conversion (100%) and low-conversion (15%) samples were measured. The low-conversion reactions contained 25 mM Hepes, pH 7, 12 mM L-malate-2-*h*(*d*), 30 mM $MgSO_4$, and 10 mM NAD, in a total volume of 33 mL. The high-conversion sample contained the same components, with the exception that the concentration of L-malate-2-*h*(*d*) was 2 mM. The reaction mixtures were adjusted to pH ~6 and sparged with CO_2 free nitrogen for at least 3 h. The pH was then adjusted to 8.2 with KOH, and the mixture was sparged for an additional 2 h. The high-conversion reaction was initiated by the addition of 0.6 mg of wild type malic enzyme and the reaction was allowed to incubate overnight. The completeness of the reaction was determined by taking an aliquot of the sample mixture and determining the absorbance at 340 nm. The low-conversion reaction was initiated by the addition of one of the mutant enzymes. The progress of the reaction was checked by measuring the absorbance of the aliquots at 340 nm. All the reactions were quenched by the addition of 100 μL of concentrated sulfuric acid prior to CO_2 isolation. The $^{12}C/^{13}C$ ratio of the isolated CO_2 was determined using an isotope ratio mass spectrometer (Finnigan Delta E). All ratios were corrected for ^{17}O according to Craig (*18*).

Data Analysis. Initial velocity data were fitted with BASIC versions of the FORTRAN programs developed by Cleland (*19*). Saturation curves for malate, NAD, and the metal ion were fitted using eq 1. Data conforming to an equilibrium ordered or sequential kinetic mechanism were fitted using eqs 2 and 3, while data for competitive inhibition were fitted to eq 4.

$$v = \frac{VA}{K_a + A} \tag{1}$$

$$v = \frac{VAB}{K_{ia}K_b + K_aB + K_bA + AB} \tag{2}$$

$$v = \frac{VAB}{K_{ia}K_b + K_aB + K_bA + AB} \tag{3}$$

$$v = \frac{VA}{K_a\left(1 + \frac{I}{K_{is}}\right) + A} \tag{4}$$

In eqs 1−4, v represents the initial velocity, V is the maximum velocity, A and B are the reactant concentrations, K_a and K_b are the Michaelis constants for A and B, K_{ia} is the inhibition constant for A, and K_{is} is the slope inhibition constant.

Data for primary kinetic deuterium isotope effects were fitted using eq 5, where F_i is the fraction of deuterium in the labeled compound, and $E_{V/K}$ and E_V are the isotope effects minus 1 on V/K and V, respectively.

$$v = \frac{VA}{K_a(1 + F_iE_{V/K}) + A(1 + F_iE_V)} \tag{5}$$

^{13}C isotope effects were calculated using eq 6, where f is the fraction of completion of reaction, and R_f and R_0 are the $^{12}C/^{13}C$ isotopic ratios of CO_2 at low and high conversion representing the ratio in the substrate, respectively. Isotope ratios are measured as $\delta^{13}C$, eq 7, where R_{smp} and R_{std} are $^{12}C/^{13}C$ isotopic ratios for sample and standard, respectively. The standard for CO_2 was Pee Dee Belemnite (*18*) with $^{12}C/^{13}C$ of 0.011 237 2.

$$^{13}\left(\frac{V}{K}\right) = \frac{\log(1 - f)}{\log\left(1 - f\left[\frac{R_f}{R_0}\right]\right)} \tag{6}$$

$$\delta^{13}C = (R_{smp}/R_{std} - 1) \times 1000 \tag{7}$$

Calculation of Intrinsic Isotope Effects and Commitment Factors. Estimates of intrinsic isotope effects and commitment factors were obtained according to Karsten and Cook (*16*, *20*) using an iterative method to search for the best fit. Wild type *A. suum* malic enzyme has a stepwise mechanism (*20*, *21*) with the requirement that the metal ion must bind to the enzyme prior to malate (*8*, *9*, *22*). The kinetic mechanism may be described as in eq 8, where M is Mg^{2+}, A is oxidized dinucleotide, B is L-malate, X is enzyme-bound oxaloacetate intermediate and R is reduced dinucleotide.

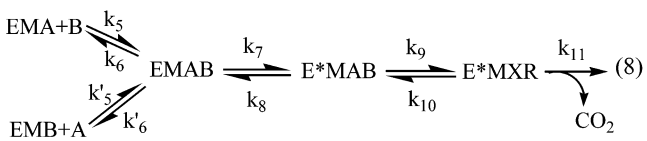

(8)

Since this is a random kinetic mechanism, the rate constants k_5 and k_6 are for the malate-binding and release at saturating concentrations ($10K_m$) of NAD and Mg^{2+}, and the rate constants k_5' and k_6' are for the dinucleotide-binding and release at saturating malate and Mg^{2+}. The rate constants k_7 and k_8 represent any precatalytic conformational change leading to a Michaelis complex, while k_9 and k_{10} are for hydride transfer, and k_{11} represents decarboxylation. There is likely no binding site for CO_2, and thus the release of CO_2 is likely very fast (*9*, *22*) and the decarboxylation step

Table 1: Kinetic Parameters for the N479 Mutant Enzymes

parameter	wild type	N479Q	N479S
K_{malate} (mM)	0.8 ± 0.1	1.8 ± 0.2	1.7 ± 0.3
fold increase		2.2 ± 0.4	2.1 ± 0.5
K_{NAD} (mM)	0.032 ± 0.004	0.034 ± 0.005	0.057 ± 0.009
fold increase		1.1 ± 0.2	1.8 ± 0.3
V/E_t (s^{-1})	31 ± 1	$(20 \pm 1) \times 10^{-3}$	$(15 \pm 1) \times 10^{-3}$
fold decrease		1500 ± 100	2000 ± 150
$V/(K_{malate}E_t)$ (M^{-1} s^{-1})	$(3.8 \pm 0.5) \times 10^4$	11 ± 1	8.8 ± 0.2
fold decrease		3500 ± 500	4300 ± 500
$V/(K_{NAD}E_t)$ (M^{-1} s^{-1})	$(1.0 \pm 0.2) \times 10^6$	600 ± 80	260 ± 60
fold decrease		1700 ± 400	3800 ± 1000

is practically irreversible. On the basis of this mechanism, the equations for the isotope effects are as follows:

$$^{D}\left(\frac{V}{K_{malate}}\right) = \frac{^{D}k_9 + c_f + {}^{D}K_{eq}(c_r)}{1 + c_f + c_r} \quad (9)$$

$$^{13}\left(\frac{V}{K_{malate}}\right)_H = \frac{^{13}k_{11} + \left(\frac{1 + c_f}{c_r}\right)}{1 + \left(\frac{1 + c_f}{c_r}\right)} \quad (10)$$

$$^{13}\left(\frac{V}{K_{malate}}\right)_D = \frac{^{13}k_{11} + \left(\frac{1 + c_f/{}^{D}k_9}{{}^{D}K_{eq}(c_r)/{}^{D}k_9}\right)}{1 + \left(\frac{1 + c_f/{}^{D}k_9}{{}^{D}K_{eq}(c_r)/{}^{D}k_9}\right)} = \frac{^{13}k_{11} + \left(\frac{^{D}k_9 + c_f}{^{D}K_{eq}(c_r)}\right)}{1 + \left(\frac{^{D}k_9 + c_f}{^{D}K_{eq}(c_r)}\right)} \quad (11)$$

The commitment factors are relative to the hydride transfer step, where c_f is the forward commitment to catalysis, $(k_9/k_8)(1 + k_7/k_6)$, and c_r is the reverse commitment to catalysis (k_{10}/k_{11}). The intrinsic primary kinetic deuterium isotope effect is $^{D}k_9$, while $^{l3}k_{11}$ is the intrinsic primary kinetic ^{13}C isotope effect. $^{D}K_{eq,}$ $^{D}k_9/^{D}k_{10}$, is the deuterium isotope effect on the equilibrium constant which was determined by Cook et al. as 1.18 (*23*).

Assuming a concerted mechanism, the intrinsic isotope effects and forward commitment factor were calculated according to Weiss et al. (*21*). The kinetic mechanism is illustrated in eq 12 where M, A, and B are as defined in eq 8.

$$EMA + B \underset{k_6}{\overset{k_5}{\rightleftharpoons}} EMAB \underset{k_8}{\overset{k_7}{\rightleftharpoons}} E^*MAB \xrightarrow{k_9} CO_2 \quad (12)$$

The rate constants k_5, k_6, k_7, and k_8 are as defined for eq 8. The rate constant k_9 is for the concerted oxidative decarboxylation step. For this mechanism, the equations for the isotope effects are as follows:

$$^{D}\left(\frac{V}{K_{malate}}\right) = \frac{^{D}k_9 + c_f}{1 + c_f} \quad (13)$$

$$^{13}\left(\frac{V}{K_{malate}}\right)_H = \frac{^{13}k_9 + c_f}{1 + c_f} \quad (14)$$

$$^{13}\left(\frac{V}{K_{malate}}\right)_D = \frac{^{13}k_9 + \frac{c_f}{^{D}k_9}}{1 + \frac{c_f}{^{D}k_9}} \quad (15)$$

The c_f term is as for eq 8, while c_r is zero for this mechanism and does not appear in the equations. All other terms are as defined for eq 8.

RESULTS

Initial Velocity Studies. In order to characterize the mutant enzymes, initial rate studies were carried out. Initial velocity patterns were obtained by measuring the initial rate as a function of NAD at different concentrations of malate and with metal ion maintained at saturation ($10K_m$). Kinetic parameters are summarized in Tables 1 and 2.

Asparagine-479, which interacts with the carboxamide side chain of NAD, as shown in Figure 2, was mutated to glutamine, serine, and methionine.[2] A 2-fold increase in K_{malate} was observed for the Q and S mutant enzymes, Table 1. The N479Q mutant enzyme exhibited no significant change in K_{NAD}, while the N479S mutant gave only a 2-fold increase. However, both mutant enzymes had significantly reduced values of V/E_t (> 10^3-fold). Inhibition constants for NADH, as a competitive inhibitor vs NAD, were 15 and 17 μM, respectively, for the N479Q and N479S mutant enzymes compared to a value of 19 μM for the wild type enzyme. Mutations of N479 thus affect the catalytic pathway, which includes the conformational change to close the site in preparation for catalysis, hydride transfer, and decarboxylation.

Serine-433 and asparagine-434 interact with the nicotinamide ribose of NAD, Figure 2. In addition, N434 interacts with β-carboxylate of malate. Table 2 lists the kinetic parameters for the S433 and N434 mutant enzymes. All of the mutant enzymes, with the exception of S433C, exhibited modest changes in K_{malate}. The S433C mutant enzyme exhibited apparent 9- and 500-fold increases in K_{malate} and K_{NAD}, respectively. (Since the enzyme could not be saturated with NAD, kinetic parameters were not determined). The S433A mutant enzyme showed an 80-fold increase in K_{NAD}. The N434Q and M mutant enzymes exhibited modest changes in K_{NAD}, while the N434A mutant enzyme showed a slight decrease in K_{NAD}. Replacing the β-hydroxyl of serine with a β-thiol as in cysteine gave an enzyme with a very high apparent K_{NAD} (16 mM), which made it impossible to determine V/E_t and $V/K_{malate}E_t$, but $V/K_{NAD}E_t$ decreased significantly (3×10^5-fold), likely as a result of the bulky sulfur causing crowding. In agreement, V/E_t and $V/K_{malate}E_t$ decreased only 6-fold and 10-fold, respectively, for the S433A mutant enzyme when the β-hydroxyl group was replaced by a hydrogen compared to wild type enzyme. More pronounced effects were observed for the N434 mutant

[2] The kinetic parameters for the N479M mutant enzyme could not be determined because of its estimated 10^5-fold decreased activity.

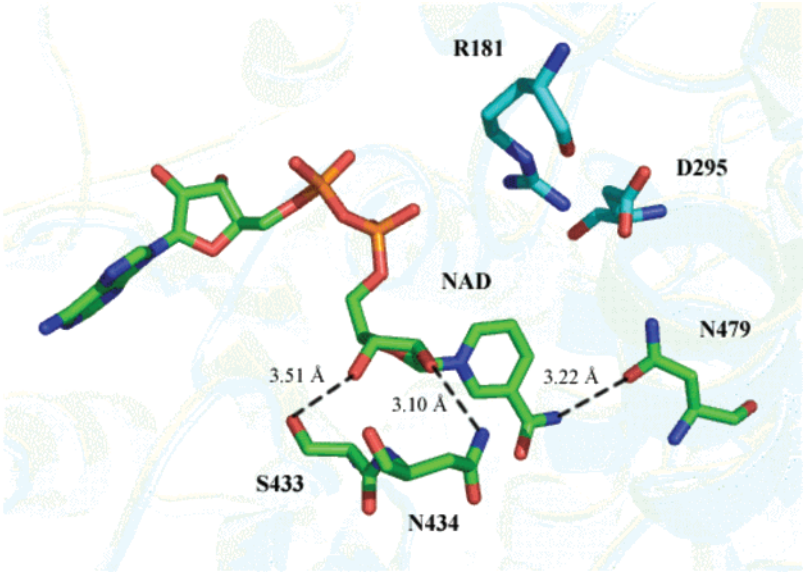

FIGURE 2: Close-up of the binding site for NAD (PDB code 1llq) in the *Ascaris* malic enzyme and the residues that interact with the cofactor and their hydrogen-bonding distances. This figure was generated using the PyMOL molecular visualization program (website: http://pymol.sourceforge.net/).

Table 2: Kinetic Parameters for the S433 and N434 Mutant Enzymes

parameter	wild type	S433A	N434Q	N434M	N434A
K_{malate} (mM)	0.8 ± 0.1 [0.24 ± 0.08][a]	1.3 ± 0.3	4.3 ± 0.5	2.2 ± 0.7	[0.50 ± 0.03][a]
fold increase		1.6 ± 0.5	5 ± 1	3 ± 1	2 ± 0.7
K_{NAD} (mM)	0.032 ± 0.004 [0.07 ± 0.01][a]	2.6 ± 0.3	0.08 ± 0.02	0.23 ± 0.06	[0.050 ± 0.008][a]
fold increase		80 ± 15	2.5 ± 0.7	7 ± 2	1.4 ± 0.3[b]
V/E_t (s^{-1})	31 ± 1 [45 ± 4][a]	5.3 ± 0.2	$(2.2 \pm 0.2) \times 10^{-3}$	$(2.8 \pm 0.2) \times 10^{-3}$	[$(1.30 \pm 0.05) \times 10^{-2}$][a]
fold decrease		6 ± 0.3	$14\,000 \pm 1\,500$	$10\,000 \pm 1\,000$	$3\,500 \pm 350$
$V/(K_{malate}E_t)$ (M^{-1} s^{-1})	$(3.8 \pm 0.5) \times 10^4$ [$(1.9 \pm 0.6) \times 10^5$][a]	$(4.0 \pm 0.3) \times 10^3$	0.51 ± 0.04	0.64 ± 0.04	[3.0 ± 0.1][a]
fold decrease		10 ± 1	$75\,000 \pm 11\,000$	$30\,000 \pm 9\,000$	$63\,000 \pm 20{,}000$
$V/(K_{NAD}E_t)$ (M^{-1} s^{-1})	$(1.0 \pm 0.2) \times 10^6$ [$(6.5 \pm 1.0) \times 10^5$][a]	$(2.0 \pm 0.2) \times 10^3$	28.0 ± 0.3	6.1 ± 0.3	[260 ± 60][a]
fold decrease		500 ± 100	$35\,000 \pm 7\,000$	$75\,000 \pm 30\,000$	2500 ± 700

[a] Values in brackets are kinetic parameters with Mn^{2+}. [b] Fold decrease.

Table 3: Primary Deuterium and ^{13}C Kinetic Isotope Effects for the Wild Type and Mutant Malic Enzymes

	^{D}V	$^{D}(V/K_{malate})$	$^{13}(V/K)_H$	$^{13}(V/K)_D$
wild type	2.0 ± 0.2 (2.1 ± 0.2)[c]	1.6 ± 0.3 (1.8 ± 0.1)	1.0342 ± 0.0002[a] (1.0353 ± 0.0005)[c]	1.0252 ± 0.0001[a,b] (1.02348 ± 0.00008)[c]
N479Q	1.8 ± 0.1	2.0 ± 0.2	1.0235 ± 0.0015	1.0250 ± 0.0007[d]
N479S	1.8 ± 0.1	1.5 ± 0.3	1.0313 ± 0.0032	1.0242 ± 0.0003[b]
S433A	2.8 ± 0.8	2.1 ± 0.2	1.0300 ± 0.0032	1.0166 ± 0.0001[b]
S433C	ND[e]	1.8 ± 0.1	1.0200 ± 0.0001	1.0129 ± 0.0015[b]
N434A	(1.9 ± 0.1)	(1.77 ± 0.15)[f]	(1.0447 ± 0.0006)	(1.030 ± 0.001)
N434M	1.03 ± 0.16	1.08 ± 0.74	ND[e]	ND[e]

[a] Values from Weiss et al. (*21*). [b] Stepwise mechanism applying $[(^{13}(V/K)_H - 1)/(^{13}(V/K)_D - 1)] = [(^{D}(V/K))/(^{D}K_{eq})]$. [c] Values in parantheses are isotope effects with Mn^{2+} from Karsten et al. (*27*). [d] Concerted mechanism. [e] ND is for not determined ($K_{NAD} = 16$ mM). [f] Calculated value using the equations for a concerted mechanism.

enzymes which gave more than a 10^3-fold decrease in V/E_t, $V/K_{malate}E_t$, and $V/K_{NAD}E_t$. The inhibition constant for NADH for the S433 and N434 mutant enzymes could not be accurately determined but was greater than 0.3 mM in all cases.

Isotope Effect Studies. Kinetic deuterium isotope effects, ^{D}V and $^{D}(V/K_{malate})$, were determined by direct comparison of initial velocities for the wild type and mutant malic enzymes at saturating concentrations ($10K_m$) of metal ion and NAD, varying L-malate-2-(*h*,*d*). $^{13}(V/K)_H$ and $^{13}(V/K)_D$ were also determined as described in the Materials and Methods section. The values of ^{D}V and $^{D}(V/K_{malate})$ are the mean averages of at least six separate determinations, and the effects are equal to one another for all mutant enzymes (with the possible exception of S433A) within error. All results are listed in Table 3. No significant change in ^{D}V or $^{D}(V/K_{malate})$ compared to the wt was observed for the N479Q and S and the N434A mutant enzymes. ^{D}V and $^{D}(V/K)$ may have increased slightly for S433A, while both values were unity, within error, for N434M.

Primary ^{13}C kinetic isotope effects decreased for all mutant enzymes compared to the wild type enzyme, with the

exception of N434A. $^{13}(V/K)_D$ values were smaller than the $^{13}(V/K)_H$ values, indicating that the mechanism is stepwise for all mutant enzymes, with the exception of N479Q mutant enzyme (see footnote *d* in Table 3). In the case of N479Q, $^{13}(V/K)_H = {}^{13}(V/K)_D$ indicates a concerted mechanism.

DISCUSSION

The purpose of this study was to investigate the function of the residues that interact with the nicotinamide and ribose rings of the dinucleotide substrate. Site-directed mutagenesis, initial rate kinetics, and isotope effects were used to probe the contribution of these groups to binding energy and catalysis.

Kinetic Parameters of the N479Q, S Mutant Enzymes. The mutant enzymes show a 2-fold increase in K_{malate}, which is indicative of a decrease in affinity. The K_m is equal to K_d for the malic enzyme, given the equality of ^DV and $^D(V/K_{malate})$ (*24*). A maximum 2-fold change in K_{NAD} is observed, even though N479 interacts with NAD, suggesting it provides only modest affinity for the cofactor, while K_{iNADH} does not change. Conformational changes are induced upon binding of NAD and malate (*13*), so it is not surprising that the affinity for both NAD and malate are affected, although only slightly. The main effect of the mutation, however, is a $>10^3$-fold decrease in V/E_t and V/KE_t for both substrates. The likely reason for this is a change in the orientation of the nicotinamide ring relative to C2 of malate as a result of hydrogen-bonding to the longer side chain of Q compared to N in the case of N479Q and the lack of the hydrogen bond for N479S. This will be discussed further below.

Isotope Effects. Data for the wild type malic enzyme indicate a stepwise mechanism with hydride transfer preceding decarboxylation (*13*). ^DV and $^D(V/K_{malate})$ values measured for the N479 mutant enzymes are similar to those of the wild type enzyme, Table 3. Although V/E_t has decreased by $>10^3$-fold, it appears at face value that the contribution of the hydride transfer to rate limitation is similar to the wild type enzyme. In the case of a stepwise mechanism, the ^{13}C isotope effect measured with L-malate-*2-d* will be lower than that observed with L-malate, as found for the wild type enzyme (*25*). For the N479Q mutant enzyme, $^{13}(V/K)_H$ and $^{13}(V/K)_D$ are equal within error, which indicates the mechanism has become concerted, with hydride transfer and decarboxylation taking place in the same step, and that the step is completely rate-limiting for the reaction. Converting asparagine to glutamine conserves the functional group, but the glutamine side chain is a methylene longer than that of asparagine. When the asparagine to glutamine mutation is modeled using PyMOL molecular visualization software, it is observed that the glutamine side chain clashes with both NAD and malate. In order to accommodate the longer side chain of glutamine, which comes into close proximity of the nicotinamide ring and malate, the position of malate and/or the nicotinamide ring relative to one another would be expected to change. In this case, malate may already be in the proper conformation for decarboxylation to occur as it is oxidized to oxaloacetate, generating more favorable molecular orbital overlap as the π bond is formed at C2−C3. That is, the oxaloacetate intermediate may either not exist or have a very short lifetime.

The change from stepwise to concerted oxidative decarboxylation is not unprecedented for the NAD−malic enzyme reaction. Multiple isotope effect studies with a variety of alternative dinucleotide substrates were measured for the malic enzyme (*20*, *21*). When NAD and NADP were used as substrates, the mechanism was stepwise, with oxidation preceding decarboxylation. The mechanism changed to concerted with the more oxidizing 3-APAD(P), 3-PAAD, and thio-NAD(P). For the stepwise mechanism, malate binds such that its C4 carboxylate is in the C2−C3 plane, which does not favor decarboxylation, and it is slow as suggested by the ^{13}C isotope effect of 1.034 measured for the wt enzyme (*21*). With the alternative, more oxidizing dinucleotide substrates, the hydride transfer step contributes more to rate limitation, resulting in a very short lifetime (no potential energy well) for the oxaloacetate intermediate. The result is an asynchronous concerted reaction with cleavage of the C3−C4 bond lagging behind C−H bond cleavage (*26*). In the case of the N479Q mutant enzyme, either an asynchronous oxidative decarboxylation takes place as observed for the wt enzyme with more oxidizing dinucleotide substrates or malate is bound with its β-carboxyl group already out of the C1−C2−C3 plane and trans to the hydride to be transferred to C4 of the nicotinamide ring of the dinucleotide, i.e., a true concerted reaction. Given the intrusion of the glutamine side chain into the malate and NAD sites, it is likely that a change in conformation of the bound malate has occurred for the N479Q mutant enzyme, placing the β-carboxyl in a better position for decarboxylation as C2 is oxidized.

Table 4: Commitment Factors and Intrinsic Isotope Effects

	c_f	c_r	$^Dk_9$	^{13}k
wild type	7[a]	14[a]	11[a]	1.052[a]
	(1)[b,c]	(2.2)[b,c]	(4)[b,c]	(1.069)[b,c]
N479Q	NA[d]	NA[d]	2.2	1.026
N479S	8.2	15	11	1.050
S433A	3	5	10	1.050
S433C	8	6	11	1.050
N434A	(1)[c]	(3)[c]	(4)[c]	(1.07)[c]

[a] Values from Karsten et al. (*20*). [b] Values from Karsten et al. (*27*). [c] Values in parantheses are with Mn^{2+}. [d] NA is not applicable.

A quantitative analysis, on the basis of theory presented in the Materials and Methods section, was used to generate estimates of forward and reverse commitment factors, intrinsic deuterium, and ^{13}C isotope effects, Table 4. For the wild type malic enzyme, the forward and reverse commitment factors are high, suggesting a significant contribution of the precatalytic conformational change to rate limitation and a partitioning of the oxaloacetate intermediate in favor of malate. For the N479Q mutant enzyme, the mechanism is concerted, and the equality of $^{13}(V/K)_H$ and $^{13}(V/K)_D$ indicates oxidative decarboxylation is completely rate limiting. The estimated intrinsic deuterium isotope effect is smaller than that observed for the wild type enzyme, as is the intrinsic ^{13}C isotope effect. The ^{13}C kinetic isotope effect of 1.025 compared to the value of 1.05 for the intrinsic ^{13}C isotope effect for decarboxylation of the oxaloacetate intermediate suggests a transition state with about 50% C2−H and C3−C4 bond cleavage if the mechanism is truly concerted.

If the above interpretation concerning the N479Q mutant enzyme is correct, the smaller serine side chain would be expected to behave differently. For the N479S mutant

enzyme, the primary deuterium and ^{13}C isotope effects are very similar to those of the wt enzyme. Deuteration of malate causes the ^{13}C isotope effect to decrease, indicating a stepwise mechanism for the N479S mutant enzyme and the data adhere to the equality for a stepwise mechanism, with oxidation preceding decarboxylation. However, there is still a $>10^3$-fold decrease in V/E_t, suggesting the nicotinamide ring must be bound differently. When the asparagine to serine mutation is modeled using PyMOL molecular visualization software, it is observed that the hydrogen-bonding interaction between this residue and the nicotinamide ring of NAD is lost, since the serine functional group is shorter than that of asparagine. None of the possible orientations of NAD or serine residue could generate a reasonable hydrogen-bonding distance. This situation likely results in an increased freedom of rotation of the nicotinamide ring, giving nonproductively bound cofactor, with a small fraction (~0.05% on the basis of V/E_t) of the dinucleotide productively bound. In agreement with this suggestion, the relative rates of steps within the catalytic pathway (precatalytic conformational change, hydride transfer, and decarboxylation), relative to one another, are similar to the wild type enzyme. (This is also supported by the estimates of the commitment factors and intrinsic isotope effects, which are very similar to those of the wild type).

Kinetic Parameters for S433 and N434 Mutant Enzymes. In order to obtain information on the interactions with the nicotinamide ribose, S433 was mutated to A and C, while N434 was mutated to Q, A, and M. Both residues hydrogen-bond to the nicotinamide ribose, Figure 2. N434 also interacts with β-carboxylate of malate.

All of the mutant enzymes exhibit a slight increase in K_{malate}, which indicates a decrease in affinity, considering the very similar values of ^DV and $^D(V/K_{malate})$ (*24*). (^DV could not be determined for the S433C mutant enzyme, but it likely behaves as the others). The S433A mutant enzyme exhibits an 80-fold increase in K_{NAD}. Because the only difference between S and A is the loss of the hydrogen bond donor, data suggest S433 provides significant binding affinity for NAD. With the use of a value of 80 for the fold change, $\Delta\Delta G^{\circ\prime}$ is 2.6 kcal/mol ($\Delta\Delta G^{\circ\prime} = RT \ln[(K_{NAD})_{S433A}/(K_{NAD})_{wt}]$). For the S433C mutant enzyme, replacement of the β-hydroxyl of S433 with the larger thiol gives a 500-fold increase in the apparent K_{NAD}, about 6-fold higher than that observed with the S to A mutation. The large increase in K_{NAD} likely results from crowding by the larger thiol, which changes the position of the bound NAD ribose, translating into a change in position of the nicotinamide ring. The inhibition constant for NADH for the S433 and N434 mutant enzymes could not be accurately determined but was greater than 0.3 mM in all cases. V/E_t and V/KE_t could not be determined for the S433C mutant enzyme because of the high value of K_{NAD}. However, the apparent $V/K_{NAD}E_t$ decreased 300 000-fold compared to the wild type and this likely includes a decrease in V/E_t and an increase in K_{NAD}.

When mutations at N434 are modeled using PyMOL software, the longer glutamine and methionine side chains stick into the active site, in close proximity to the bound malate, which likely results in reorientation of NAD and malate. However, changes in the K_m for malate and NAD were moderate for the N434 mutant enzymes, suggesting that the affinity for reactants was not altered. Nonetheless, V/E_t decreased on the order of 10^3-10^4 with the smallest change observed for N434A.

Isotope Effects. In the case of the S433A mutant enzyme, the loss of a hydrogen-bonding interaction results in a large decrease in V/E_t, suggesting a change in the orientation of the nicotinamide ring relative to C2 of malate. A slight increase in ^DV and $^D(V/K)$, coupled to a slight decrease in the ^{13}C isotope effect, suggests a change in the partitioning of the oxaloacetate intermediate favors decarboxylation, i.e., a decrease in c_r; a lower value of c_r is calculated, Table 4. A decrease in the forward commitment factor was also estimated, Table 4. All of the mutant enzymes have similar intrinsic deuterium and ^{13}C isotope effect values compared to the wild type, suggesting similar transition states for the hydride transfer and decarboxylation. All of the S433 and N434 mutant enzymes exhibited a smaller value of ^{13}C isotope effect with deuterated malate, consistent with a stepwise mechanism.

Data for the S433C mutant enzyme exhibit a $^D(V/K)$ value similar to that of the wt, while there is a decrease in the ^{13}C isotope effect. Data suggest a change in the partitioning of the oxaloacetate intermediate to favor decarboxylation. In agreement, the estimated value of c_r has decreased considerably, compared to the wt.

In addition to its interaction with the nicotinamide ribose, N434 also interacts with the β-carboxylate of malate. If the interaction is eliminated, the positioning of malate may change, resulting in changes in the rates of hydride transfer and decarboxylation. ^DV and $^D(V/K)$ values for the N434A mutant enzyme are equal, within error, to the wild type values, while $^{13}(V/K)_H$ is greater than that of the wt enzyme. Data suggest a more rate-limiting decarboxylation. The commitment factors and the intrinsic isotope effects were almost identical to the wt values. However, 3 500-fold decrease in V/E_t suggests that only a small fraction of the dinucleotide is productively bound, as for N479S. The rates of the steps within the catalytic pathway slow down with the same ratio relative to one another.

In the case of the N434M mutant enzyme, the longer methionine side chain sticks into the active site, in close proximity to C4 of malate, likely causing a change in the orientation of malate and slowing down decarboxylation. The ^{13}C isotope effects were not determined for this mutant enzyme since V/E_t decreased 10 000-fold. However, it would be expected that ^DV and $^D(V/K_{malate})$, unity within error, most likely reflect the decarboxylation step becoming totally rate-limiting. Isotope effects were not determined for the N434Q mutant enzyme since the rate was too low (14 000-fold decrease in V/E_t).

Conclusions. Results obtained for the N479 mutant enzymes indicate that the hydrogen bond donated by N479 to the carboxamide side chain of the nicotinamide ring is crucial for proper orientation in the hydride transfer step of the *Ascaris* NAD−malic enzyme reaction. This is very reasonable if one considers the structure of the enzyme.

S433 and N434 residues are very important in positioning the dinucleotide. Data obtained for all mutant enzymes suggest the following: (1) The orientation of the nicotinamide is very strictly controlled, because any mutation, whether it is conservative or not, caused considerable decrease in the rate of the reaction. (2) S433 provides significant binding affinity for NAD, and its replacement with

A generates significant nonproductive binding of the cofactor. (3) The effect of N434 mutant enzymes is more pronounced in terms of the positioning of NAD and malate. (4) Differences in the dissociation constants for NAD and NADH indicate the enzyme sees the oxidized and reduced forms of the cofactor differently.

ACKNOWLEDGMENT

We thank Dr. William E. Karsten for his invaluable help in his technical support and interpretation of data.

REFERENCES

1. Ochoa, S., Mehler, A. H., and Kornberg, A. (1947) Reversible oxidative decarboxylation of malic acid, *Fed. Proc. 6*, 282.
2. Hsu, R. Y., and Lardy, H. A. (1967) Pigeon liver malic enzyme 2. Isolation, crystallization and some properties, *J. Biol. Chem. 242*, 520−526.
3. Karsten, W. E., and Cook, P. F. (2000) Pyridine nucleotide-dependent beta-hydroxyacid oxidative decarboxylases: An overview, *Protein Pept. Lett. 7*, 281−286.
4. Saz, H. J., and Hubbard, J. A. (1957) The oxidative decarboxylation of malate by *Ascaris lumbricoides*, *J. Biol. Chem. 225*, 921−933.
5. Saz, H. J. (1971) Anaerobic phosphorylation in *Ascaris* mitochondria and effects of Anthelmintics, *Comp. Biochem. Physiol. 39*, 627−637.
6. Seidman, I., and Entner, N. (1961) Oxidative enzymes and their role in phosphorylation in sarcosomes of adult *Ascaris lumbricoides*, *J. Biol. Chem. 236*, 915−919.
7. Saz, H. J. (1981) Energy metabolisms of parasitic helminths-Adaptations to parasitism, *Annu. Rev. Physiol. 43*, 323−341.
8. Park, S. H., Kiick, D. M., Harris, B. G., and Cook, P. F. (1984) Kinetic mechanism in the direction of oxidative decarboxylation for NAD−malic enzyme from *Ascaris suum*, *Biochemistry 23*, 5446−5453.
9. Chen, C. Y., Harris, B. G., and Cook, P. F. (1988) Isotope partitioning for NAD malic enzyme from *Ascaris suum* confirms a steady-state random kinetic mechanism, *Biochemistry 27*, 212−219.
10. Kiick, D. M., Harris, B. G., and Cook, P. F. (1986) Protonation mechanism and location of rate-determining steps for the *Ascaris suum* nicotinamide adenine dinucleotide−malic enzyme reaction from isotope effects and pH studies, *Biochemistry 25*, 227−236.
11. Park, S. H., Harris, B. G., and Cook, P. F. (1986) pH-dependence of kinetic parameters for oxalacetate decarboxylation and pyruvate reduction reactions catalyzed by malic enzyme, *Biochemistry 25*, 3752−3759.
12. Karsten, W. E., Liu, D. L., Rao, G. S. J., Harris, B. G., and Cook, P. F. (2005) A catalytic triad is responsible for acid−base chemistry in the *Ascaris suum* NAD−malic enzyme, *Biochemistry 44*, 3626−3635.
13. Rajapaksa, R., Abusoud, H., Raushel, F. M., Harris, B. G., and Cook, P. F. (1993) Pre-steady-state kinetics reveal a slow isomerization of the enzyme−NAD complex in the NAD−malic enzyme reaction, *Biochemistry 32*, 1928−1934.
14. Karsten, W. E., Chooback, L., Liu, D., Hwang, C. C., Lynch, C., and Cook, P. F. (1999) Mapping the active site topography of the NAD-malic enzyme via alanine-scanning site-directed mutagenesis, *Biochemistry 38*, 10527−10532.
15. Bradford, M. M., and Williams, W. L. (1976) New, rapid, sensitive method for protein determination, *Fed. Proc. 35*, 274.
16. Karsten, W. E., and Cook, P. F. (2007) The multiple roles of arginine-181 in binding and catalysis in the NAD-malic enzyme from *Ascaris suum*, *Biochemistry 46*, 14578−14588.
17. O'Leary, M. H. (1980) Determination of heavy-atom isotope effects on enzyme-catalyzed reactions, *Methods Enzymol. 64 (Enzyme Kinet. Mech., Part B)*, 83−104.
18. Craig, N. (1957) Isotopic standards for carbon and oxygen and correction factors for mass-spectrometric analysis of CO_2, *Geochim. Cosmochim. Acta 12*, 133−140.
19. Cleland, W. W. (1979) Statistical analysis of enzyme kinetic data, *Methods. Enzymol. 63 (Enzyme Kinet. Mech., Part A)*, 103−138.
20. Karsten, W. E., and Cook, P. F. (1994) Stepwise versus concerted oxidative decarboxylation catalyzed by malic enzyme: A reinvestigation, *Biochemistry 33*, 2096−2103.
21. Weiss, P. M., Gavva, S. R., Harris, B. G., Urbauer, J. L., Cleland, W. W., and Cook, P. F. (1991) Multiple isotope effects with alternative dinucleotide substrates as a probe of the malic enzyme reaction, *Biochemistry 30*, 5755−5763.
22. Mallick, S., Harris, B. G., and Cook, P. F. (1991) Kinetic mechanism of NAD-malic enzyme from *Ascaris suum* in the direction of reductive carboxylation, *J. Biol. Chem. 266*, 2732−2738.
23. Cook, P. F., Blanchard, J. S., and Cleland, W. W. (1980) Primary and secondary deuterium isotope effects on equilibrium constants for enzyme-catalyzed reactions, *Biochemistry 19*, 4853−4858.
24. Klinman, J. P., and Matthews, R. G. (1985) Calculation of substrate dissociation constants from steady-state isotope effects in enzyme-catalyzed reactions, *J. Am. Chem. Soc. 107*, 1058−1060.
25. Hermes, J. D., Roeske, C. A., O'Leary, M. H., and Cleland, W. W. (1982) Use of multiple isotope effects to determine enzyme mechanisms and intrinsic isotope effects. Malic enzyme and glucose-6-phosphate dehydrogenase, *Biochemistry 21*, 5106−5114.
26. Edens, W. A., Urbauer, J. L., and Cleland, W. W. (1997) Determination of the chemical mechanism of malic enzyme by isotope effects, *Biochemistry 36*, 1141−1147.
27. Karsten, W. E., Gavva, S. R., Park, S. H., and Cook, P. F. (1995) Metal ion activator effects on intrinsic isotope effects for hydride transfer and decarboxylation in the reaction catalyzed by the NAD−malic enzyme from *Ascaris suum*, *Biochemistry 34*, 3253−3260.

BI702261M